古 脊 椎 动 物 学 报
VERTEBRATA PALASIATICA

DOI: 10.19615/j.cnki.2096-9899.230901

Reappraisal of *Bothriolepis sinensis* Chi, 1940 from the Tiaomachien Formation, Hunan, China

LUO Yan-Chao[1,2] ZHU Min[1,2] LU Li-Wu[3] PAN Zhao-Hui[1*]

(1 *Key Laboratory of Vertebrate Evolution and Human Origins of Chinese Academy of Sciences*, *Institute of Vertebrate Paleontology and Paleoanthropology*, *Chinese Academy of Sciences* Beijing 100044)
(2 *University of Chinese Academy of Sciences* Beijing 100049 * Corresponding author: panzhaohui@ivpp.ac.cn)
(3 *Geological Museum of China* Beijing 10034)

Abstract *Bothriolepis sinensis* Chi 1940, mainly based on anterior median dorsal plates from the Middle Devonian Tiaomachien Formation of Hunan, is the first Paleozoic vertebrate taxon erected in China. Although additional materials of *B. sinensis* from the type locality were described by Lu in 1988, its morphology and phylogeny remain poorly understood. In this study, we complemented the morphology of the skull and trunk armor of *B. sinensis* based on Chi's specimens housed in the Institute of Vertebrate Paleontology and Paleoanthropology, Chinese Academy of Sciences, and several previously undescribed specimens in the Geological Museum of China. *Bothriolepis sinensis* differs from other *Bothriolepis* in the following combination of characteristics: enlarged supraotic thickening, length/width ratio of head shield 1.4–1.6, broad orbital fenestra (greater than 1/3 of the head shield width), and fan-shaped preorbital recess. The phylogenetic analysis did not place *B. askinae* in the most basal position of the genus and revealed that *B. sinensis* and *B. kwangtungensis* consistently from a monophyletic group characterized by their slender proximal segment of the pectoral fin (length/width ratio greater than 7). A majority of Chinese *Bothriolepis* species (*B. niushoushanensis*, *B. lochangensis*, *B. tungseni*, *B. kwangtungensis* and *B. sinensis*) were clustered in a clade characterized by the pectoral pit-line on the ventral central plate 1 extending to the ventral central plate 2. The paleogeographic reconstruction using the data from the DeepBone platform showed that *Bothriolepis* had its oldest occurrences in South China and East Gondwana in Eifelian, dispersed rapidly worldwide, and then diversified across the coasts of the Rheic Ocean.

Key words Hunan, Middle Devonian, Antiarcha, *Bothriolepis*, phylogeny, paleobiogeography, data visualization

Citation Luo Y C, Zhu M, Lu L W et al., in press. Reappraisal of *Bothriolepis sinensis* Chi, 1940 from the Tiaomachien Formation, Hunan, China. Vertebrata PalAsiatica. DOI: 10.19615/j.cnki.2096-9899.230901

国家自然科学基金(批准号：42002015, 41872023, 42130209, 42272028), 中国科学院青年创新促进会(编号：2021070)和古生物学与地层学国家重点实验室(编号：193121)资助。

收稿日期：2022-05-08

1 Introduction

The Antiarcha is a group of placoderms that first appeared in the Ludlow (late Silurian) and became extinct in the Late Devonian (Moy-Thomas and Miles, 1971; Wang, 1991; Carr, 1995; Janvier, 1996; Zhao et al., 2016). As a diverse group in the Devonian, the Antiarcha is characterized by its highly specialized dermal armor pattern, especially the pectoral fin and the head shield (Goujet and Young, 1995; Janvier, 1996). Recent phylogenetic studies (Brazeau, 2009; Davis et al., 2012; Zhu et al., 2013, 2016; Dupret et al., 2014; Giles et al., 2015; Long et al., 2015; Qiao et al., 2016) placed the Antiarcha at or near the most basal position of placoderms and made it a keenly watched early vertebrate group (Zhu M et al., 2012; Giles et al., 2013; Long et al., 2015; Trinajstic et al., 2015; Charest et al., 2018; Wang and Zhu, 2018, 2021; Zhu Y A et al., 2021, 2022).

Bothriolepis, one of the earliest known Paleozoic vertebrate taxa among placoderms (Eichwald, 1840; Miller, 1841), was distributed worldwide. *Bothriolepis sinensis* was the first Paleozoic vertebrate taxon erected in China (Chi, 1940), mainly based on three specimens of the anterior median dorsal plate (AMD) found by Chi Y S in 1937. These specimens were collected from the Middle Devonian Tiaomachien Formation (also spelled as Tiaomajian Formation) in Changsha, Hunan (Chi, 1940; Pan, 1958, 1959; Pan and Dineley, 1988; Wang, 1984; Zhao and Zhu, 2010; Qie et al., 2019, Fig. 1). Later, Pan and colleagues collected additional materials of *B. sinensis* and made some complementary descriptions (Pan, 1959; Lu, 1988). However, these descriptions in Chinese were overlooked by other researchers for a

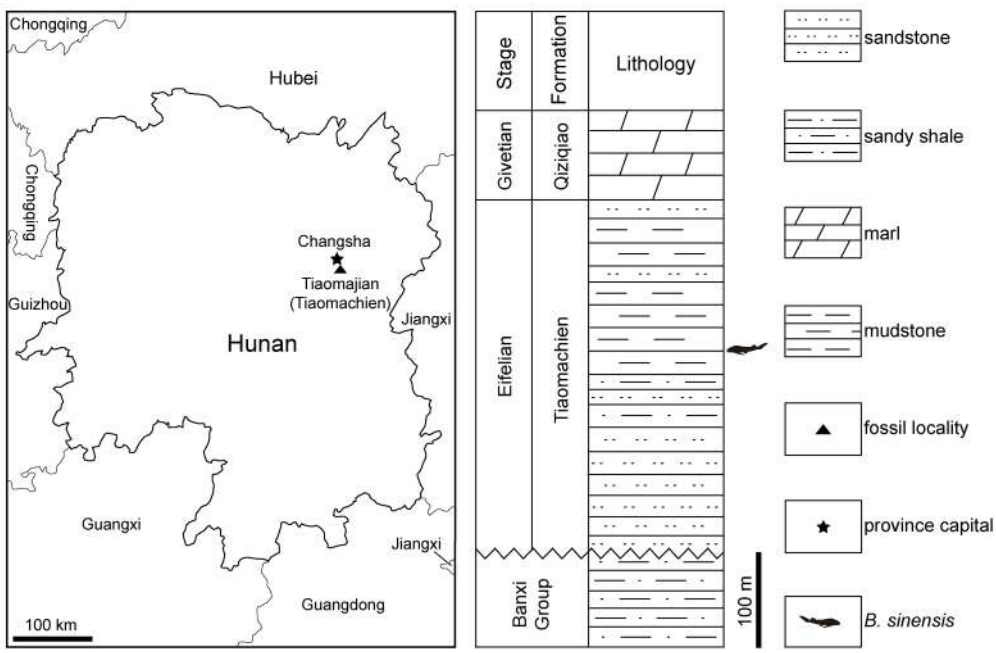

Fig. 1 Map of the fossil site and the fish-bearing horizon in this study
Based on: GS(2019)3266

long time, resulting in the phylogenetic affinity of *B. sinensis* unsettled. Here we redescribe the holotype of *B. sinensis* and other available specimens from Chi's collection housed in IVPP, and additional specimens housed in GMC. We also established a relatively comprehensive matrix comprising 77 taxa (75 *Bothriolepis* species and 2 outgroups) and 69 characters to discuss the interrelationships of *Bothriolepis*. Based on the data from DeepBone (www.deepbone.org, Pan and Zhu, 2019) and Scotese's paleogeographic reconstructions (Scotese et al., 2021), we also explore the temporal and spatial distribution of *Bothriolepis*.

2 Material and methods

To explore the phylogeny of *Bothriolepis*, we chose *Grossilepis tuberculata* (Lukševičs, 1996) and *Dianolepis liui* (Chang, 1965; Pan et al., 2018), two bothriolepidoid species as the out-groups. We compiled a matrix containing 75 *Bothriolepis* species, 2 outgroups, and 69 characters (see "*Bothriolepis* dataset" matrix in Supplementary Information) using Mesquite v.3.61 (Maddison, 2019) and performed the phylogenetic analysis using TNT v.1.5 (Goloboff and Catalano, 2016). In the phylogenetic analysis, we excluded 11 *Bothriolepis* species that have a rate of character coding completeness of less than 10% (see Supplementary Information) to get a more resolved result. The characters and codings are mainly based on Long (1983), Lukševičs (2001, 2021), Young (2010), and Dupret et al. (2023). All characters are set as unordered.

Institutional abbreviations IVPP, Institute of Vertebrate Paleontology and Paleoanthropology, Chinese Academy of Sciences, Beijing, China; GMC, Geological Museum of China, Beijing, China.

Anatomical abbreviations ADL, anterior dorsolateral plate; AMD, anterior median dorsal plate; alr, postlevator thickening of anterior median dorsal plate; a.PrL, attachment area for prelateral plate; a_1SM, anterior attachment area for submarginal plate; a_2SM, posterior attachment area for submarginal plate; $CD_{1–3}$, dorsal central plate 1–3; cf.ADL, area overlapping anterior dorsolateral plate; cf.AMD, area overlapping anterior median dorsal plate; cf.MxL, area overlapping mixilateral plate; cr.pm, paramarginal crista of head shield; cr.pto, postorbital crista of head shield; cr.tp, posterior internal transverse crista; cr.tv, transverse nuchal crista of head shield; fm, insertion fossa on head shield for levator muscles; f.retr, levator fossa of anterior median dorsal plate; g, pit on postpineal plate; grm, ventral median groove on dorsal wall of trunk shield; L, lateral plate; $ML_{2–3}$, lateral marginal plate 2–3; $MM_{2–3}$, mesial marginal plate 2–3; MxL, mixilateral plate; mvr, ventral median ridge of anterior median dorsal plate; Nu, nuchal plate; nprl, prelateral notch of head shield; oa.AMD, area overlapped by anterior median dorsal plate; oa.AVL, area overlapped by anterior ventrolateral plate; oa.PMD, area overlapped by posterior median dorsal plate; oa.PVL, area overlapped by posterior ventrolateral plate; ood, otic-occipital depression of head shield; PM, postmarginal plate; PMD, posterior median dorsal plate; PNu, paranuchal plate; PP, postpineal plate; PrM, premedian plate; PVL, posterior ventrolateral plate; p, lateral pit of head shield; pr.dm,

median dorsal process of mixilateral plate; prh, preorbital recess of head shield; pro, obstantic process of trunk shield; proc, preobstantic corner of head shield; pr.po, depression on head shield for dorsal face of the endocranial postorbital process; prv1, anterior ventral process of anterior median dorsal plate; pt1, anterior ventral pit of dorsal wall of anterior median dorsal plate; sot, supraotic thickening of head shield; tlg, transverse lateral groove of head shield paleoanthropology.

3 Systematic paleontology

Class Placodermi McCoy, 1848
Order Antiarcha Cope, 1885
Suborder Euantiarcha Janvier & Pan, 1982
Infraorder Bothriolepidoidei Gross, 1965
Family Bothriolepidae Miles, 1968
Genus *Bothriolepis* Eichwald, 1840
***Bothriolepis sinensis* Chi, 1940**

(Figs. 2–5)

Bothriolepis sinensis Chi, 1940, p. 57–73, pl. I, figs. 1–7; text-fig. 3

Bothriolepis sinensis Pan, 1959, p. 27–28, pl. IV, figs. 1, 2

Bothriolepis sinensis Lu, 1988, p. 69–77, pl. I, fig. 1; pl. II, figs. 1–4; text-figs. 1–4

Holotype IVPP V467a, internal mould of an AMD (Chi, 1940:pl. I-1).

Referred specimens IVPP V467b, internal mould of an ADL (Chi, 1940:pl. I-7); V467c, internal mould of an incomplete AMD (Chi, 1940:pl. I-3); V467d, internal mould of a MxL (Chi, 1940:pl. I-5); GMV1961, internal mould of a head shield, articulating with part of the trunk shield (Lu, 1988:fig. 1, pl. I-1); GMV1972, a complete proximal segment of pectoral fin (Pan, 1959:pl. I-2); GMV1974a, an incomplete proximal segment of pectoral fin (Lu, 1988:pl. III-1); GMV1974b, external mould of an incomplete distal segment of pectoral fin; GMV1975, a PrM.

Diagnosis (emended) *Bothriolepis sinensis* resembles *B. shaokuanensis* in the broad orbital fenestra (greater than 1/3 of the head shield width) and slender pectoral fin (length/width ratio greater than 7). *Bothriolepis sinensis* can be characterized by its enlarged supraotic thickening of the head shield (longer than half of the nuchal plate); length/width ratio of the head shield 1.4–1.6; fan-shaped preorbital recess; similar length and width of the PrM; high transverse nuchal crista; length/width ratio of AMD about 1.5; ventral median ridge reaching the anterior margin of AMD; high anterior ventral process; AMD overlapped by MxL.

4 Description

The head shield itself was largely eroded except the PrM (Fig. 2B). The PrM is broad, with its width and length nearly equal, and its anterior margin 1.5 times its posterior margin.

The radiation center of ornamentation is visible on the anterior margin of the preorbital recess (prh, Fig. 2B). A round-shaped poriferous area on the visceral side of the PrM is located at the anterior one-fourth of the plate and engages the anterior margin of the preorbital recess, resembling some Australian *Bothriolepis* species such as *B. askinae* and *B. karawaka* (Young, 1988). A similar feature can be also found in some other antiarch genera like *Livnolepis* (Moloshnikov, 2004, 2008), however, the poriferous area in the latter is a narrow lozenge that does not reach the anterior margin of the preorbital recess.

Thanks to the complete internal mould of the head shield, visceral details of the head shield are preserved (Fig. 2). An enlarged lateral pit on the lateral plate (p, Fig. 2B) is visible anteriorly of the transverse lateral groove of head shield (tlg, Fig. 2B). Young (1988) discussed the large lateral pit in some of the "Victorian species" without clear identification criteria. Here we regard lateral pits that are larger than the minimum width of the transverse lateral groove as large lateral pits, as in *B. sinensis*. But the lateral pit of *B. sinensis* is still much smaller than that of *B. barretti* (Young, 1988). The transverse lateral groove runs between the anterior and the posterior attachment areas for submarginal plate (a_1SM, a_2SM, Fig. 2B). The anterior attachment area is placed anterolaterally to the transverse lateral groove (Fig. 2B), and the posterior attachment area extends posteriorly behind the preobstantic corner (proc, Fig. 2B), similar to *B. macphersoni* (Young, 1988). The lateral and posterolateral margins of the head shield form a 145° angle at the preobstantic corner, as in *B. shaokuanensis* (Chang, 1965) and *B. niushoushanensis* (Pan et al., 1980, 1987). A pit (g, Fig. 2B) is present on the postpineal plate. The attachment area for prelateral plate (a.PrL, Fig. 2B) lies at the anterolateral margin of the

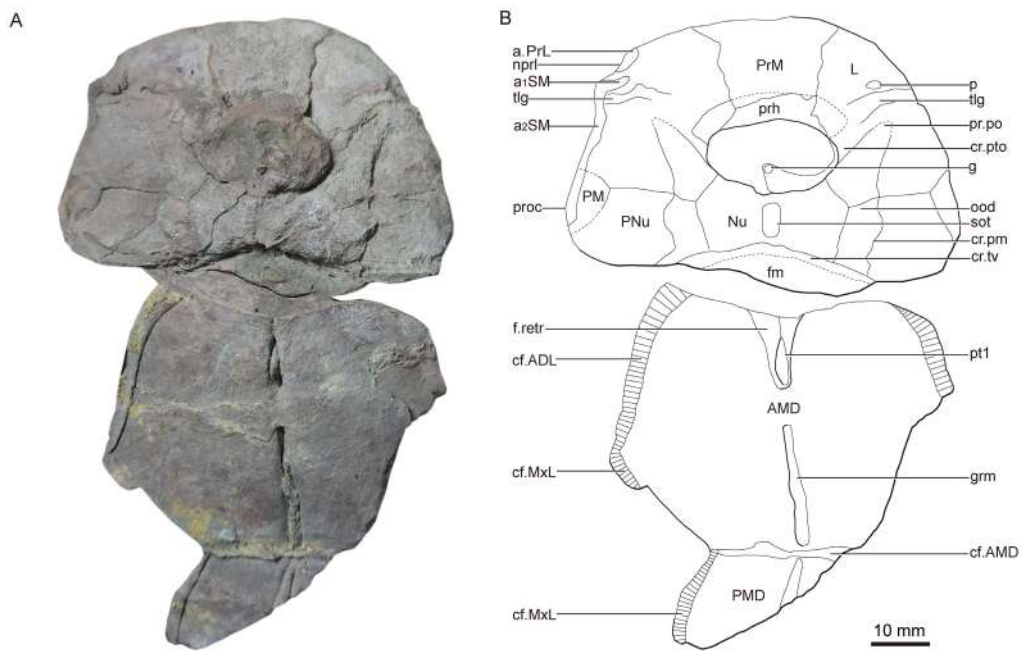

Fig. 2 Photo (A) and illustrative drawing (B) of the referred specimen of *Bothriolepis sinensis* (GMV1961)

PM (Fig. 2B). The preorbital recess is fan-shaped, which Lu (1988) considered as a transitional form between “trilobate” type (e.g., *B. nitida*, Leidy, 1856; Young, 1988; Thomson and Thomas, 2001) and “simple” type (e.g., *B. askinae*, Young, 1988). The otic-occipital depression (ood, Fig. 2B) shows that the dorsal face of the endocranial postorbital process (pr.po, Fig. 2B) reaches the level of the anterior margin of the orbital fenestra. The transverse nuchal crista (cr.

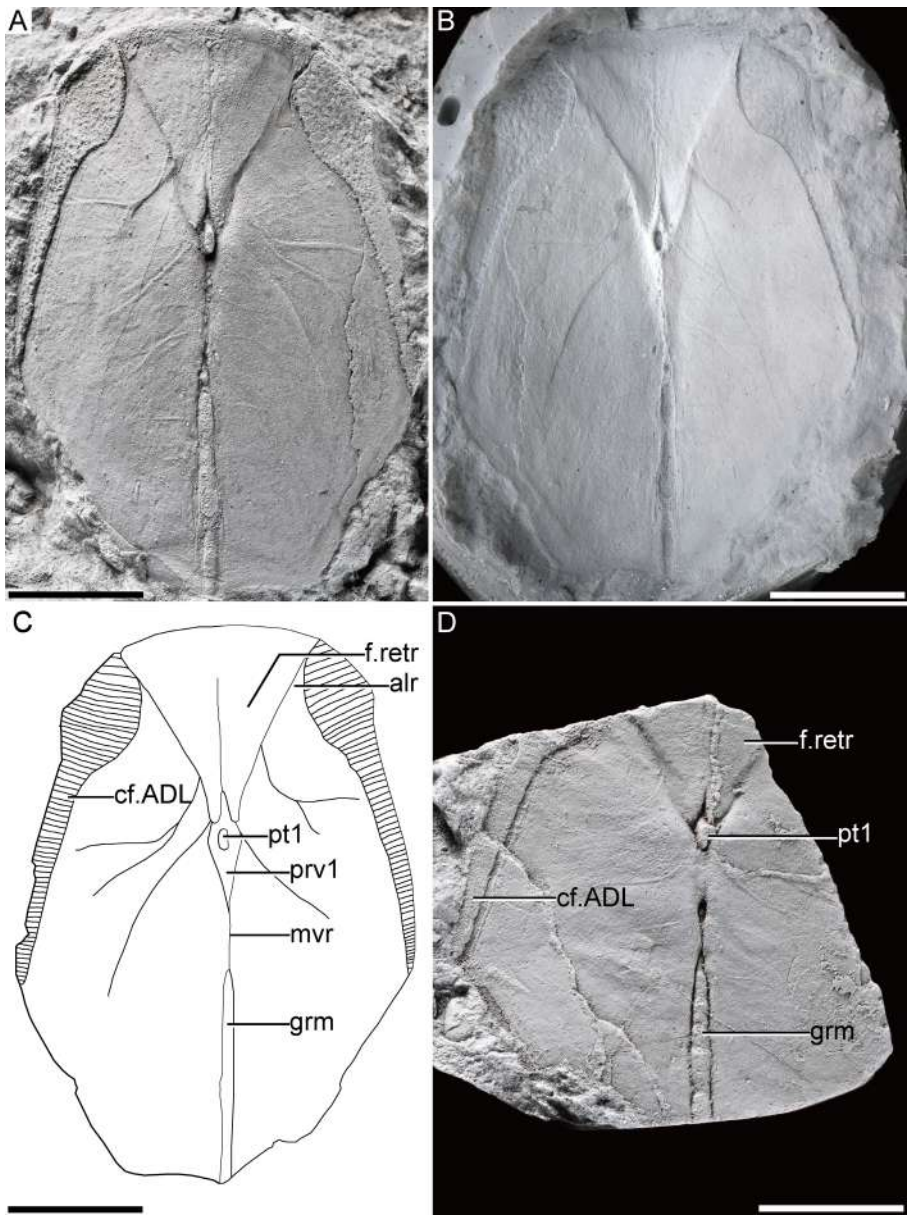

Fig. 3 Anterior median dorsal plate of *Bothriolepis sinensis*
A. photo of the internal mould of AMD (IVPP V467a, Chi, 1940:pl. I-1); B, C. photo and illustrative drawing of AMD (V467a) in ventral view; D. internal mould of AMD (V467c, Chi, 1940:pl. I-3)
A and D are coated with ammonium chloride. Scale bars = 10 mm

tv, Fig. 2B) is high and protrudes anteriorly. The unpaired insertion fossa on the head shield for levator muscles (fm, Fig. 2B) is relatively large, and reaches half the length of the PNu (Fig. 2B). The supraotic thickening (sot, Fig. 2B) is present on the visceral side of the Nu (Fig. 2B), and its size is much larger than that in other *Bothriolepis* species (Long and Werdelin, 1986; Young, 1988; Johanson; 1997; Moloshnikov, 2009; Downs et al., 2016).

The holotype IVPP V467a shows a visceral aspect of AMD (Fig. 3A–C). The length/width ratio is about 1.5. The anterior ventral process and pit (prv1, pt1, Fig. 3C) are located at the anterior two-thirds of the midline. The index between the width of the anterior margin and the maximum width of AMD is about 1.6, and the index between the anterior and posterior divisions of the AMD is about 1.5. The area overlapping ADL (cf.ADL, Fig. 3C) is on the anterolateral margin of the AMD. The levator fossa and postlevator thickening of AMD (f.retr, alr, Fig. 3C) are situated on the anterior portion of the plate. The MxL overlaps the AMD completely in the holotype and IVPP V467c. However, in GMV1961 the AMD bears an area overlapping the MxL (cf.MxL, Fig. 2B) that occupies one-third of the posterolateral margin of AMD, representing the individual variation. The ventral median groove of the AMD (grm, Fig. 3C) runs behind the ventral median ridge (mvr, Fig. 3C) and extends into the PMD. The PMD is incomplete, and its length/width ratio remains unknown.

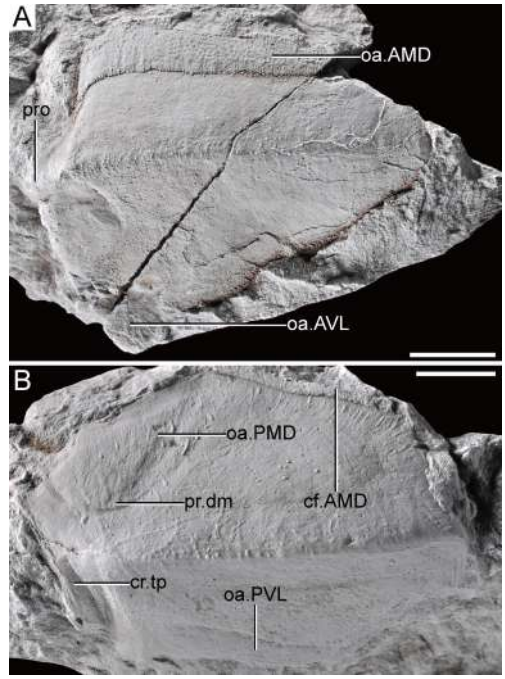

Fig. 4 Other referred specimens of *B. sinensis* collected by Chi in the 1930s
A. internal mould of the left ADL (IVPP V467b, Chi, 1940:pl. I-7); B. internal mould of the right MxL (V467d, Chi, 1940:pl. I-5). Fossils are whitened with ammonium chloride
Scale bars = 10 mm

The ADL is preserved as an incomplete internal mould (Fig. 4A), which was previously referred to as an indeterminable dermal bone (Chi, 1940:pl. I-7). The dorsal lamina is 42 mm long by 14 mm wide, and the lateral lamina is 21 mm wide. The angle between the dorsal and lateral laminae is about 120°. The area overlapped by the AMD (oa.AMD, Fig. 4A) is on the dorsal margin, and the fragmented area overlapped by the AVL (oa.AVL, Fig. 4A) is on its ventral margin. A well-developed but short obstantic process (pro, Fig. 4A) on the anterior margin of the ADL only extends one-fifth of the total length of the plate, similar to *B. fergusoni* (Long and Werdelin, 1986).

The MxL (Fig. 4B) is well preserved as an internal mould, which was previously referred to as an ADL (Chi, 1940:pl. I-5). The dorsal lamina is 42 mm long by 18 mm wide, and the

lateral lamina is 14 mm wide. The angle between the dorsal and lateral laminae is about 135°. A strong posterior internal transverse crista (cr.tp, Fig. 4B) is placed posteriorly. The area overlapping AMD (cf.AMD, Fig. 4B) is on the anterior dorsal margin, with depressions that mark the areas overlapped by PMD (oa.PMD, Fig. 4B) and PVL (oa.PVL, Fig. 4B). The median dorsal process of MxL is low and lacks an obtrusive corner, suggesting that the PMD bears a rounded lateral corner.

The pectoral fin specimens are well preserved to show the proximal and distal segments. The proximal segment is slender, with the length/width ratio greater than 7. In GMV1974a, the proximal segment is 78 mm long by 11 mm wide. The distal segment of the pectoral fin is preserved as an incomplete external mould in GMV1974b. The contact relationships of distal segment plates remain unknown. Spines are present on the lateral margins of lateral marginal plate 2 (ML_2, Fig. 5) and distal segment.

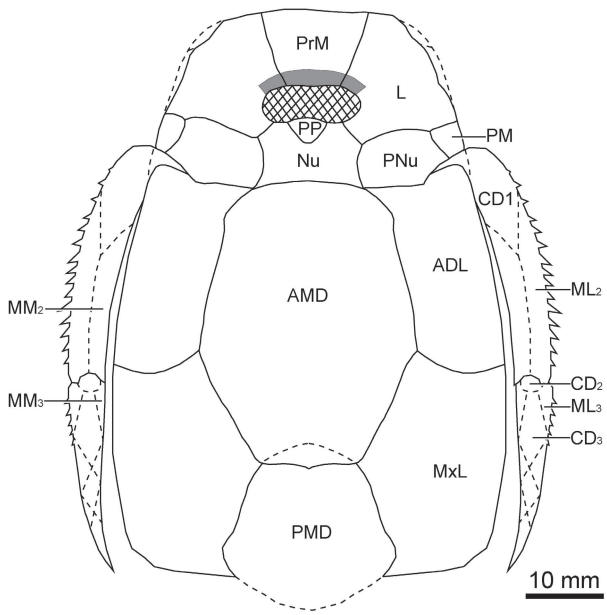

Fig. 5 Reconstruction of *Bothriolepis sinensis*

5 Discussion

5.1 Interrelationships of *Bothriolepis*

The phylogeny of *Bothriolepis* has received attention for decades. A few studies (Long, 1983; Lukševičs, 2001; Young, 2010) that discussed the interrelationships of *Bothriolepis* only used synapomorphies to show their phylogeny without any parsimony analysis. Dupret et al. (2023) compiled a character matrix based on previous studies, which contains a majority of the *Bothriolepis* species, but the outgroup he used for the analysis (*B. askinae*) was not suitable for resolving the interrelationships of *Bothriolepis*. Following Long (1983), Lukševičs

(2001), Young (2010), and Dupret et al. (2023), we established a more comprehensive matrix to discuss the interrelationships of *Bothriolepis*. Our phylogenetic analysis yielded 264 most parsimonious trees of length 324, with a consistency index (CI) of 0.235, and a retention index (RI) of 0.507. The low CI represents extensive convergences and reversals (Qiao and Zhu, 2015). Though the strict consensus tree is poorly resolved, reflecting the inherent difficulties in resolving the interrelationships of *Bothriolepis*, we can still extract phylogenetic signals for the paleobiogeographic discussion.

Our study disagrees with Young (1988), Lukševičs (2001), and Dupret et al. (2023) in that *B. askinae* is not placed in the most basal position of the genus. The clade (Node 1, Fig. 6) contains all *Bothriolepis* species and is supported by two synapomorphies: anterior and posterior edges of orbitonasal fenestra straight and parallel (Character 7, state 0); semi-circular groove on lateral plate developed (Character 60, state 1). We agree Lukševičs (2001) in that *B. prima* and *B. obrutschewi* form a clade (Node 2, Fig. 6), which is characterized by two synapomorphies: the posterior margin of orbit anterior to the junction formed by lateral, postmarginal and paranuchal plates (Character 11, state 0), and the junction of rostral infraorbital sensory line in midline on PrM straight or with a weak posterior indentation (Character 59, state 0). A majority of the Chinese species (*B. niushoushanensis*, *B. lochangensis*, *B. tungseni*, *B. kwangtungensis*, and *B. sinensis*) in our research are placed in the same clade (Node 3, Fig. 6) by a synapomorphy that the pectoral pit-line on the ventral central

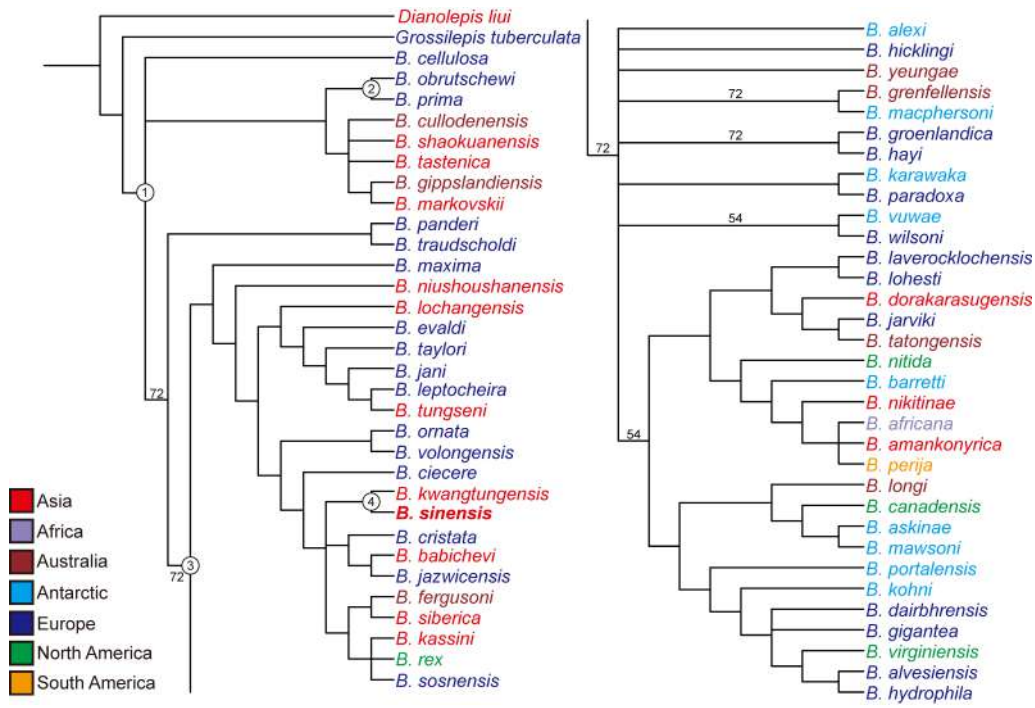

Fig. 6 The 50% majority rule consensus tree of 264 most parsimonious trees, shows the phylogenetic position of *B. sinensis* within *Bothriolepis*
Numbers on the branches display the majorities which do not reach 100

plate 1 extending to the ventral central plate 2 (Character 66, state 1). Besides, *B. sinensis* and *B. kwangtungensis* form a monophyletic group (Node 4, Fig. 6) by their slender proximal segment of the pectoral fin (length/width ratio greater than 7, Character 50, state 1). These four clades (Nodes 1–4, Fig. 6) are both manifested by a suboptimal tree that is retained in Bremer supports analysis (retain trees suboptimal by 100), which represents considerable stability.

5.2 Paleobiogeography of *Bothriolepis*

The cosmopolitan antiarch *Bothriolepis* is one of the most diverse genera in placoderms (Fig. 7A). Moreover, *Bothriolepis* exhibits some features that reveal endemic signals, e.g., the trilobate preorbital recess only appears in the Antarctic species (Young, 1988); the trifid preorbital recess appears in the species from Greenland (Stensiö, 1948), Europe (Miles, 1968), and Australia (Long and Werdelin, 1986); and the fan-shaped preorbital recess only appears in the Chinese species (Chi, 1940; Pan, 1959; Pan et al., 1980; Lu, 1988).

Here we used the data from DeepBone (Pan and Zhu, 2019) to perform the data visualization. We converted the latitude and longitude coordinates of these fossil sites into pixel coordinates of raster tile maps using the Web Mercator algorithm (Fig. 7A). To reveal the paleobiogeography of *Bothriolepis*, we plotted these fossil sites on each paleo map by the paleogeographic coordinate calculations (PointTrack version 7.0) and reconstructions (Scotese, 2002; Ke et al., 2016; Pan et al., 2022) (Fig. 7B). The general trend of radiation in *Bothriolepis* is from South China and

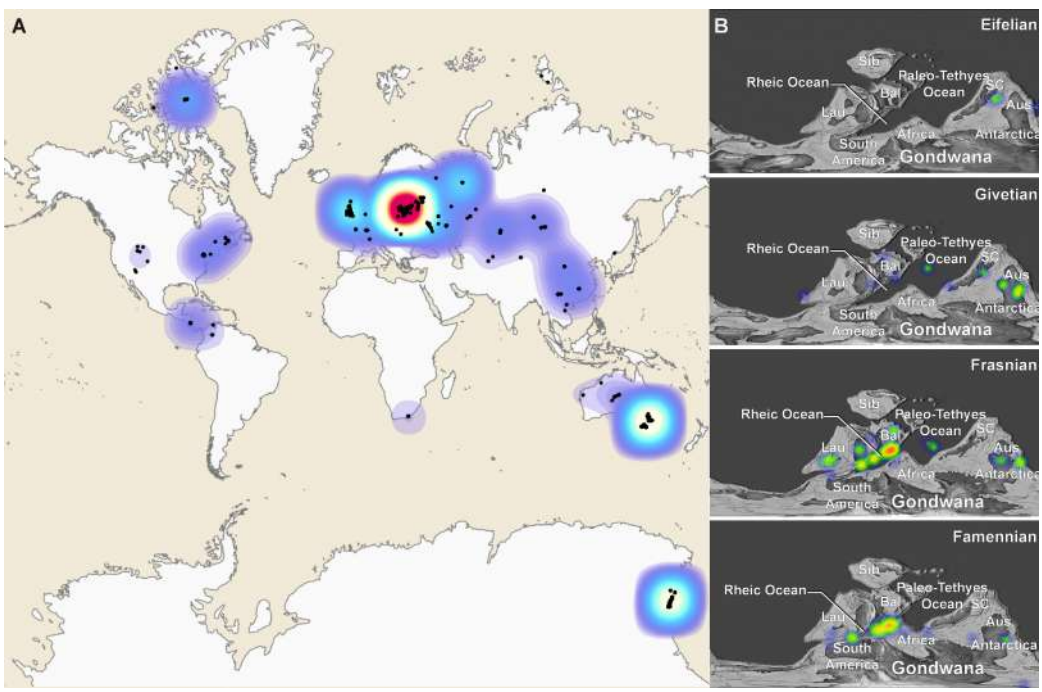

Fig. 7 Geographical distribution of *Bothriolepis*

A. fossil sites of *Bothriolepis*; B. paleobiogeography of *Bothriolepis* based on Scotese's paleogeographic reconstructions. Abbreviations: Aus, Australia; Bal. Baltica; Lau. Laurentia; SC. South China; Sib. Siberia

East Gondwana to the coasts of the Rheic Ocean (Fig. 7B). The specimens we counted in the Deepbone database included 106 taxa of *Bothriolepis* (75 species and their specimens with solid identification, location, and horizon information; 31 specimens were considered indeterminate, but their localities can still be used in the calculation of geographical distribution).

Two *Bothriolepis* species, *B. verrucose* (Young and Gorter, 1981) and *B. yunnanensis* (Liu, 1962; Zhao and Zhu, 2010) that showed the most early-diverging forms of *Bothriolepis*, appeared in South China and East Gondwana (Australia) of Eifelian (Fig. 7B), which represented the initial rise of *Bothriolepis*. *Bothriolepis* gradually became more diverse in Givetian, and multiple species (16 taxa) widely spread from the Paleo-Tethyes Ocean to the East of Australia, and Antarctica (Fig. 7B). The migration of *Bothriolepis* was kept westwards in Frasnian. 35 species of *Bothriolepis* from Australia, the Paleo-Tethyes Ocean, Baltica, and Laurentia were described for this stage (Fig. 7B). In Famennian, 22 species of *Bothriolepis* were described on the coasts of the Rheic Ocean, which were South America, Africa, Baltica, and Laurentia. Moreover, sporadic species appeared in Australia and Antarctica (Fig. 7B).

6 Conclusion

We described several additional specimens of *B. sinensis*, which included some head shields (GMV1961, GMV1975), trunk plates (GMV1961, IVPP V467), and pectoral fins (GMV1972, GMV1974). According to additional specimens, *B. sinensis* can be identified by the following characteristics: enlarged supraotic thickening, length/width ratio of head shield 1.4–1.6, broad orbital fenestra (greater than 1/3 of the head shield width), and fan-shaped preorbital recess. We also compiled a relatively comprehensive matrix containing 75 *Bothriolepis* species, 2 outgroups, and 69 characters to reveal the interrelationships of *Bothriolepis*. The phylogenetic analysis showed that *B. sinensis* and *B. kwangtungensis* form a monophyletic group by their slender proximal segment of pectoral fin. In addition, most of the Chinese species in our phylogenetic analysis (*B. niushoushanensis*, *B. lochangensis*, *B. tungseni*, *B. kwangtungensis* and *B. sinensis*) are placed in the same clade by their pectoral pit-lines on the ventral central plate 1 extending to ventral central plate 2. According to the data from the DeepBone platform, we summarized the trend of dispersal of *Bothriolepis* from South China and East Gondwana to the coasts of the Rheic Ocean.

Acknowledgments We thank Jia Lian-Tao and Cui Xin-Dong for their assistance during this work. This project was supported by the National Natural Science Foundation of China (42002015, 41872023, 42130209, 42272028), Youth Innovation Promotion Association CAS (2021070), and State Key Laboratory of Palaeobiology and Stratigraphy (Nanjing Institute of Geology and Palaeontology, CAS) (193121).

Supplementary material can be found on the website of Vertebrate PalAsiatica (http://www.vertpala.ac.cn /CN/2096-9899/home.shtml).

湖南中泥盆统跳马涧组中华沟鳞鱼再研究

罗彦超[1,2] 朱 敏[1,2] 卢立伍[3] 潘照晖[1]

(1 中国科学院古脊椎动物与古人类研究所，中国科学院脊椎动物演化与人类起源重点实验室 北京 100044)

(2 中国科学院大学 北京 100049)

(3 中国地质博物馆 北京 100034)

摘要：计荣森先生于1940年基于湖南长沙附近中泥盆统跳马涧组采集到的一些以前中背片为代表的胴甲鱼类标本命名了中华沟鳞鱼(*Bothriolepis sinensis*), 这是在中国正式命名的第一种古生代脊椎动物。虽然卢立伍于1988年对后续出产于模式种产地的其他中华沟鳞鱼材料进行了补充描述，但研究者对中华沟鳞鱼的形态学特征和系统发育仍缺乏全面认识。在此基于计荣森先生所采集的样本及一些收藏于中国地质博物馆未正式发表的化石，对中华沟鳞鱼进行了再研究，补充了其头部与躯甲的部分特征。与其他沟鳞鱼类相比，中华沟鳞鱼拥有以下一系列特征：较大的听上加厚区、颅顶甲长宽比1.4–1.6、较宽的眶窗(宽于颅顶甲的1/3)以及扇形的眶前凹等。系统发育分析结果显示，*B. askinae*并非位于沟鳞鱼支系的最原始位置；中华沟鳞鱼与广东沟鳞鱼因同样拥有纤细的附肢近端(长宽比大于7)而形成了一个稳定的单系。本研究中绝大部分的中国种类均位于同一支系上，该支系的共有衍征为其胸鳍感觉管从第一腹中片延伸至第二腹中片。此外，基于“深骨”平台数据的古生物地理可视化分析结果表明，沟鳞鱼类最早于艾菲尔期出现在华南与东冈瓦纳，并迅速地辐射并扩散至全球，最终于法门期在瑞亚克洋两岸表现出了高度的物种多样性。

关键词：湖南，中泥盆统，胴甲鱼类，沟鳞鱼类，系统发育，古生物地理学，数据可视化

References

Brazeau M D, 2009. The braincase and jaws of a Devonian ‘acanthodian’ and modern gnathostome origins. Nature, 457: 305–308

Carr R K, 1995. Placoderm diversity and evolution. Bull Mus Natl Hist Nat, Paris, 4e sér, Sec C, 17: 85–125

Chang K J, 1965. New antiarchs from the Middle Devonian of Yunnan. Vert PalAsiat, 9: 1–9

Charest F, Johanson Z, Cloutier R, 2018. Loss in the making: absence of pelvic fins and presence of paedomorphic pelvic girdles in a Late Devonian antiarch placoderm (jawed stem-gnathostome). Biol Lett, 14: 20180199

Chi Y S, 1940. On the discovery of *Bothriolepis* in the Devonian of central Hunan. Bull Geol Soc China, 20: 57–73

Cope E D, 1885. The position of *Pterichthys* in the system. Am Nat, 19: 289–291

Davis S P, Finarelli J A, Coates M I, 2012. *Acanthodes* and shark-like conditions in the last common ancestor of modern gnathostomes. Nature, 486: 247–250

Downs J P, Daeschler E B, Garcia V E et al., 2016. A new large-bodied species of *Bothriolepis* (Antiarchi) from the Upper Devonian of Ellesmere Island, Nunavut, Canada. J Vert Paleont, 36: e1221833

Dupret V, Sanchez S, Goujet D et al., 2014. A primitive placoderm sheds light on the origin of the jawed vertebrate face. Nature, 507: 500–503

Dupret V, Byrne H M, Castro N et al., 2023. The *Bothriolepis* (Placodermi, Antiarcha) material from the Valentia Slate Formation of the Iveragh Peninsula (middle Givetian, Ireland): Morphology, evolutionary and systematic considerations, phylogenetic and palaeogeographic implications. PLoS One, 18: e0280208

Eichwald E, 1840. Die Tier-und Pflanzenreste des alten roten Sandsteins und Bergkalks im Nowgorodschen Gouvernement. Saint-Petersburg Acad Imp Sci. Bull Sci, 7: 78–91

Giles S, Rücklin M, Donoghue P C J, 2013. Histology of "placoderm" dermal skeletons: Implications for the nature of the ancestral gnathostome. J Morphol, 274: 627–644

Giles S, Darras L, Clement G et al., 2015. An exceptionally preserved Late Devonian actinopterygian provides a new model for primitive cranial anatomy in ray-finned fishes. Proc R Soc B, 282: 20151485

Goloboff P A, Catalano S A, 2016. TNT version 1.5, including a full implementation of phylogenetic morphometrics. Cladistics, 32: 221–238

Goujet D F, Young G C, 1995. Interrelationships of placoderms revisited. Geobios Mém Spéc, 19: 89–95

Gross W, 1965. *Bothriolepis* cf. *panderi* Lahusen in einem Geschiebe von Travemünde bei Lübeck. Mitt Geol Staatsinst Hamburg, 34: 138–141

Janvier P, 1996. The dawn of the vertebrates: characters versus common ascent in the rise of current vertebrate phylogenies. Palaeontology, 39: 259–287

Janvier P, Pan J, 1982. *Hyrcanaspis bliecki* n. g. n. sp., a new primitive euantiarch (Antiarcha, Placodermi) from the Middle Devonian of northeastern Iran, with a discussion on antiarch phylogeny. N J Geol Palaont Abh, 164: 364–392

Johanson Z, 1997. New antiarchs (Placodermi) from the Hunter Siltstone (Famennian) near Grenfell, N.S.W. Alcheringa, 21: 191–217

Ke Y, Shen S Z, Shi G R et al., 2016. Global brachiopod palaeobiogeographical evolution from Changhsingian (Late Permian) to Rhaetian (Late Triassic). Palaeogeogr, Palaeoclimatol, Palaeoecol, 448: 4–25

Leidy J, 1856. Descriptions of some remains of fishes from the Carboniferous and Devonian formations of the United States. J Acad Nat Sci Phila, 3: 159–165

Liu Y H, 1962. A new species of *Bothriolepis* from Yunnan. Vert PalAsiat, 6: 80–85

Long J A, 1983. New bothriolepid fish from the Late Devonian of Victoria, Australia. Palaeontology, 26: 295–320

Long J A, Werdelin L, 1986. A new Late Devonian bothriolepid (Placodermi, Antiarcha) from Victoria, with descriptions of other species from the state. Alcheringa, 10: 355–399

Long J A, Mark-Kurik E, Johanson Z et al., 2015. Copulation in antiarch placoderms and the origin of gnathostome internal fertilization. Nature, 517: 196–199

Lu L W, 1988. New data of *Bothriolepis* (Placodermi: Antiaroha) from Middle Devonian of Central Hunan, China. In: Xin Y S, Huang Z Z, Wang F Q et al. eds. Geological Museum Study. Beijing: Seismological Press. 69–77

Lukševičs E, 1996. Bothriolepid Antiarchs (Placodermi, Bothriolepididae) from the North-western Part of East European Platform. Ph. D thesis. Riga: University of Latvia. Summary

Lukševičs E, 2001. Bothriolepid antiarchs (Vertebrata, Placodermi) from the Devonian of the north-western part of the East European Platform. Geodiversitas, 23: 489–609

Lukševičs E, 2021. Revision of asterolepidoid antiarch remains from the Ogre Formation (Upper Devonian) of Latvia. Proc Est Acad Sci Geol, 70: 3–17

Maddison W P, Maddison D R, 2019. Mesquite: a modular system for evolutionary analysis. Version 3.61. Updated at http://

www.mesquiteproject.org, accessed 21 February 2021

McCoy F, 1848. On some new fossil fish from the Carboniferous Period. Ann Mag Nat Hist, 2: 1–10, 115–133

Miles R S, 1968. The Old Red Sandstone antiarchs of Scotland: Family Bothriolepididae. Palaeontogr Soc Monogr, 122: 1–130

Miller H, 1841. The Old Red Sandstone or New Walks in an Old Field. Edinburgh: John Johnstone. 1–275

Moloshnikov S V, 2004. Crested antiarch *Bothriolepis zadonica* HD Obrucheva from the Lower Famennian of Central European Russia. Acta Palaeontol Pol, 49: 135–146

Moloshnikov S V, 2008. Devonian antiarchs (Pisces, Antiarchi) from central and Southern European Russia. Paleontol J, 42: 691–773

Moloshnikov S V, 2009. New data on Late Devonian bothriolepidid placoderms (Pisces, Antiarchi) from Tuva. Paleontol J, 43: 558–568

Moy-Thomas J A, Miles R S, 1971. Palaeozoic Fishes. London: Chapman and Hall. 1–259

Pan J, 1958. On the age of Tiaomachien series of Hunan. Acta Geol Sin, 38: 135–144

Pan J, 1959. Devonian fish fossils of China and their stratigraphic and geographic distributions. Monogr Sum Basic Data Chinese Geol, 1: 23–34

Pan J, Dineley D L, 1988. A review of early (Silurian and Devonian) vertebrate biogeography and biostratigraphy of China. Proc R Soc B, 235: 29–61

Pan J, Wang S T, Liu S Y et al., 1980. Discovery of Devonian *Bothriolepis* and *Remigolepis* in Ningxia. Acta Geol Sin, 3: 175–185

Pan J, Huo F C, Cao J X et al., 1987. Continental Devonian System of Ningxia and its Biotas. Beijing: Geological Publishing House. 1–237

Pan Z H, Zhu M, 2019. VPPDB: Hosting the data for Vertebrate Paleoanthropology. Acta Geol Sin Engl Edit, 93: 61–63

Pan Z H, Zhu M, Zhu Y A et al., 2018. A new antiarch placoderm from the Emsian (Early Devonian) of Wuding, Yunnan, China. Alcheringa, 17: 1–19

Pan Z H, Niu Z B, Xian Z M et al., 2022. A novel specimen-based mid-Paleozoic dataset of antiarch placoderms (the most basal jawed vertebrates). Earth Syst Sci Data, 15: 41–51

Qiao T, Zhu M, 2015. A new Early Devonian lungfish from Guangxi, China, and its palaeogeographic significance. Alcheringa, 39: 428–437

Qiao T, King B, Long J A et al., 2016. Early gnathostome phylogeny revisited: multiple method consensus. PLoS One, 11: e0163157

Qie W K, Liang K, Königshof P, 2019. Devonian palaeoecosystems and palaeoenvironments of South China. Paleobio Paleoenv, 99: 1–5

Scotese C R, 2002. Palaeo Map Project. Available at www.scotese.com

Scotese C R, Song H, Mills B J W et al., 2021. Phanerozoic paleotemperatures: The earth's changing climate during the last 540 million years. Earth Sci Rev, 215: 103503

Stensiö E A, 1948. On the Placodermi of the Upper Devonian of East Greenland. II. Antiarchi: subfamily Bothriolepinae. With an attempt at a revision of the previously described species of that family. Medd Grønl, 139: 1–622

Thomson K S, Thomas B, 2001. On the status of species of *Bothriolepis* (Placodermi, Antiarchi) in North America. J Vert

Paleont, 21: 679–686

Trinajstic K, Boisvert C, Long J A et al., 2015. Pelvic and reproductive structures in placoderms (stem gnathostomes). Biol Rev, 90: 467–501

Wang G T, 1984. The investigation of sedimentary facies of Tiaomajian Formation in Tiaomajian Town of Changsha Country. Hunan Geol, 3: 45–56, 72

Wang J Q, 1991. The Antiarchi from Early Silurian of Hunan. Vert PalAsiat, 29: 240–244

Wang Y J, Zhu M, 2018. Redescription of *Phymolepis cuifengshanensis* (Antiarcha: Yunnanolepididae) using high-resolution computed tomography and new insights into anatomical details of the endocranium in antiarchs. PeerJ, 6: e4808

Wang Y J, Zhu M, 2021. New data on the headshield of *Parayunnanolepis xitunensis* (Placodermi, Antiarcha), with comments on nasal capsules in antiarchs. J Vert Paleont, 40: e1855189

Young G C, 1988. Antiarchs (placoderm fishes) from the Devonian Aztec Siltstone, Southern Victoria Land, Antarctica. Palaeontogr Abt A, 202: 1–125

Young G C, 2010. A new antiarch (placoderm fish: Devonian) from the south coast of New South Wales, Australia. In: Elliott D K, Maisey J G, Yu X et al. eds. Morphology Morphology, Phylogeny and Paleobiogeography of Fossil Fishes (Honoring Meemann Chang). Munich: Verlag Dr. Friedrich Pfeil. 85–100

Young G C, Gorter J D, 1981. A new fish fauna of Middle Devonian age from the Taemas/Wee Jasper region of New South Wales. Bull Bur Min Res Geol Geophys, 209: 85–147

Zhao W J, Zhu M, 2010. Siluro-Devonian vertebrate biostratigraphy and biogeography of China. Palaeoworld, 19: 4–26

Zhao W J, Zhu M, Liu S et al., 2016. A new look at the Silurian fish-bearing strata around the Shanmen Reservoir in Lixian, Hunan province. J Strat, 40: 341–350

Zhu M, Yu X B, Choo B et al., 2012. An antiarch placoderm shows that pelvic girdles arose at the root of jawed vertebrates. Biol Lett, 8: 453–456

Zhu M, Yu X B, Ahlberg P E et al., 2013. A Silurian placoderm with osteichthyan-like marginal jaw bones. Nature, 502: 188–193

Zhu M, Ahlberg P E, Pan Z H et al., 2016. A Silurian maxillate placoderm illuminates jaw evolution. Science, 354: 34–336

Zhu Y A, Giles S, Young G C et al., 2021. Endocast and bony labyrinth of a Devonian “placoderm” challenges stem gnathostome phylogeny. Curr Biol, 31: 1112–1118

Zhu Y A, Li Q, Lu J et al., 2022. The oldest complete jawed vertebrates from the early Silurian of China. Nature, 609: 954–958